View metadata, citation and similar papers at core.ac.uk

brought to you by CORE

provided by Elsevier - Publisher Connector

Journal of the American College of Cardiology Vol. 46, No. 11, 2005
© 2005 by the American College of Cardiology Foundation
Published by Elsevier Inc.
ISSN 0735-1097/05/$30.00
doi:10.1016/j.jacc.2005.08.045

PRECLINICAL STUDY

Hypoxia-Inducible Factor 1-Alpha Reduces Infarction and Attenuates Progression of Cardiac Dysfunction After Myocardial Infarction in the Mouse

Masakuni Kido, MD,* Lingling Du, MD,* Christopher C. Sullivan, MS,* Xiaodong Li, MD, PHD,* Reena Deutsch, PHD,† Stuart W. Jamieson, MB, FRCS,* Patricia A. Thistlethwaite, MD, PHD*

San Diego, California

OBJECTIVES The aim of this research was to test whether constitutive expression of hypoxia-inducible factor 1-alpha (HIF-1α) influences infarction size and cardiac performance after myocardial infarction.

BACKGROUND A major question in clinical medicine is whether infarction size and border zone remodeling of the heart can be influenced by the overexpression of specific genes in the peri-infarction region.

METHODS We investigated the role of constitutive HIF-1α expression in acute myocardial infarction using a transgenic model. Transgenic mice containing the HIF-1α gene under the control of the α-myosin heavy chain promoter were constructed. Myocardial infarction was produced by coronary ligation in HIF-1α transgenic mice and control animals. Extent of infarction was then quantitated by two-dimensional and M-mode echocardiography as well as by molecular and pathologic analysis of heart samples in infarct, peri-infarct, and remote heart regions at serial time points.

RESULTS Constitutive overexpression of HIF-1α in the murine heart resulted in attenuated infarct size and improved cardiac function 4 weeks after myocardial infarction. Significantly, we found an increase in both capillary density as well as vascular endothelial growth factor and inducible nitric oxide synthase expression in peri-infarct and infarct regions in the hearts of constitutive HIF-1α–expressing animals compared to control animals.

CONCLUSIONS These observations suggest the involvement of HIF-1α in myocardial remodeling and peri-infarct vascularization. Our results show that supranormal amounts of this peptide protect against extension of infarction and improve border zone survival in myocardial infarction. (J Am Coll Cardiol 2005;46:2116–24) © 2005 by the American College of Cardiology Foundation

Acute myocardial infarction (MI) causes approximately 2 million deaths per year (1). In acute myocardial infarction, prognosis and mortality rates are closely related to infarct size and the progression of postinfarction cardiac failure. Hypoxia-inducible factor 1 (HIF-1) is a major regulator of the hypoxic response after myocardial infarction (2). This transcription factor consists of two basic-helix-loop-helix-PAS transcription factors, HIF-1α and HIF-1β (3). HIF-1α is sensitive to hypoxia and is rapidly degraded by the ubiquitin proteasomal pathway under normoxic conditions. Decreased tissue oxygen causes altered availability of HIF-1α to the von Hippel-Lindau protein and ubiquitination, blocking its degradation (4,5). This results in nuclear accumulation of HIF-1α protein and enhancement of its transcriptional activity through binding to enhancer elements in target genes that include vascular endothelial growth factor (VEGF) (6), inducible nitric oxide synthase (iNOS) (7), erythropoietin (8), and phosphoglycerate kinase (9).

We have previously shown that the HIF-1α gene is up-regulated in regions of myocardial infarction and ischemia (2). However, the role of HIF-1α in ischemic myocardium and myocardial remodeling after infarction is unknown. To this end, we asked whether constitutive high-level expression of HIF-1α in the myocardium would influence myocardial infarction size and improve cardiac performance in the mouse after myocardial infarction.

METHODS

Transgenic mice. The pBSKII-αMHC-SV40-HIF-1α vector was constructed by subcloning the HIF-1α cDNA into the EcoRV cloning site of the pBSKII-αMHC-SV40 plasmid (gift from K. Chien, University of California, San Diego) (10). After digestion with BssHII, the fragment carrying the αMHC promoter and HIF-1α cDNA was used for microinjection into C57BL/6 zygotes. Four independent transgenic lines were established and studied. Transgenic mice were identified by PCR analysis of tail genomic DNA using the forward primer 5′-GACGGTATCGATAAGCTTGAT-3′ (derived from

From the *Division of Cardiothoracic Surgery and †Division of Biostatistics, University of California, San Diego, San Diego, California. Supported by NIH R01 HL70852 to Dr. Thistlethwaite and NIH M01 RR00827 to Dr. Deutsch. The first two authors contributed equally to this work. Douglas Losordo, MD, FACC, served as guest editor for this article.

Manuscript received February 9, 2005; revised manuscript received July 12, 2005, accepted August 1, 2005.

Abbreviations and Acronyms

EF = ejection fraction
HIF-1α = hypoxia-inducible factor 1-alpha
iNOS = inducible nitric oxide synthase
LAD = left anterior descending coronary artery
LV = left ventricle/ventricular
PCR = polymerase chain reaction
VEGF = vascular endothelial growth factor

sequence in our plasmid construct) and the reverse primer 5′-CTCGGCTAGTTAGGGTACACTTC-3′ (derived from HIF-1α sequence). To perform experiments in homozygous HIF-1α transgenic mice, we backcrossed for six generations. HIF-1α (−) mice were homozygous negative animals derived from the F2 generation. Animal experiments were performed in accordance with the protocols approved by the institutional animal care and use committee and complied with recommendations published in *Guide for the Care and Use of Laboratory Animals* (National Academic Press, Washington, DC, 1996).

Surgical procedures. Twelve-week-old male adult mice [50 HIF-1α(+) and 50 HIF-1α(−) transgenic mice] were anesthetized with 1.0% isoflurane inhalation via nose cone. A midline anterior cervical skin incision was made and the trachea exposed by sharp dissection. The trachea was intubated with a 22-gauge angiocatheter and the position of the tube was confirmed by direct visualization. Pressure-controlled ventilation (animal ventilator from Kent Scientific, Torrington, Connecticut) was initiated at 15 cm H_2O. A 1.5-cm vertical left parasternal skin incision was made, the chest cavity was entered through the fourth interspace, and the pericardium vertically opened. The left anterior descending coronary artery (LAD) was ligated with a 7-0 polypropylene suture. Ventricle blanching indicated successful occlusion of the vessel. Sham-operated animals [45 HIF-1α(+) and 45 HIF-1α(−) transgenic mice] served as surgical controls and were subjected to the same procedures as the experimental animals with the exception that the LAD was not ligated. Mortality rates during and after surgery were <2% in all groups.

Transthoracic echocardiography. Two-and-one-half-percent Avertin (2,2,2-tribromoethanol) was administered intraperitoneally at 0.01 ml/g of body weight for mild sedation. Echocardiographic analysis was performed using a commercially available echocardiograph (SONOS 5500, Philips Electronics, Amsterdam, the Netherlands) equipped with a 15-MHz linear array ultrasound transducer. The LV was assessed in both parasternal long-axis and short-axis views at a frame rate of 120 Hz. End-systole or end-diastole was defined as the phase in which the smallest or largest area of LV, respectively, was obtained. Left ventricular end-systolic diameter (LVESD) and left ventricular end-diastolic diameter (LVEDD) were measured from the LV M-mode tracing with a sweep speed of 50 mm/s at the papillary muscle level. Percentage fractional shortening (%FS) was calculated using standard formulas: $\%FS = [(LVEDD - LVESD)/LVEDD] \times 100$. Akinetic area and other cardiac parameters were also measured in the two-dimensional view both in long and short axis (11). Ejection fraction (EF) was measured by single-plane area length and calculated according to the formula: $EF\ (\%) = [(0.85\ LVAD^2/LVLD) - [0.85\ LVAS^2/LVLS)]/(0.85\ LVAD^2/LVLD) \times 100$, where LVAD = left ventricular area in end-diastole; LVAS = left ventricular area in end-systole; LVLD = left ventricular long-axis length in end diastole; and LVLS = left ventricular long-axis length in end-systole.

Morphometric determination of infarct size at 24 h or 4 weeks. Two different histologic techniques were performed to detect the extent of infarcted myocardium depending on the time after coronary artery ligation (12). First, in order to validate the accuracy of echocardiography in the noninvasive evaluation of infarct size in mouse hearts 24 h after ligation, 0.4 ml of 1% Evans blue dye in phosphate-buffered saline (PBS) was retrogradely injected into the coronary circulation to delineate the nonischemic area in 20 animals [10 HIF-1α(+) and 10 HIF-1α(−)]. Hearts were excised and rinsed in iced PBS. Six biventricular sections of 0.8 mm thickness were made perpendicular to the long axis of the heart (between the point of ligation and the apex of the heart) and incubated in 1% triphenyl tetrazolium chloride (TTC) (Sigma, St. Louis, Missouri) in PBS (pH 7.4) for 15 minutes at 37°C, fixed in 10% phosphate-buffered formalin, and digitally photographed at 10× magnification. For each slice, the area of infarction and the total area of the LV were planimetered on a 10:1 grid and reconstructed using Scion imaging software (Scion Corp., Frederick, Maryland). Area at risk (AAR) and infarct area were delineated and calculated for both sides of the section. AAR was calculated as the left ventricular area excluding Evans blue after coronary ligation. Infarct area was determined as the risk area that became necrotic as distinguished by TTC staining (TTC stains noninfarcted areas red). Infarct area was also validated by blinded histologic review of slides by a cardiac pathologist. Cumulative areas for all sections from each heart were used for comparisons.

Second, for hearts studied 4 weeks after coronary ligation [20 animals: 10 HIF-1α(+) and 10 HIF-1α(−)], organs were excised and placed in 10% phosphate-buffered formalin. The gross infarct size was measured in the intact heart by comparison of the length and width of the infarct and LV areas. The fixed tissue was embedded in paraffin and serially cut from the apex to the level just below the coronary artery ligation site. Transverse 5-μm-thick sections were cut at intervals of 500 μm, such that 14–18 sections were obtained from each heart. Alternating sections were stained with either hematoxylin/eosin or Masson trichrome. The infarcted area was measured by planimetry using Scion imaging software and expressed as a percentage of total surface area of the left ventricle. Peri-infarct (border-zone) region was defined as the 2-mm area encircling the area of pathologic infarction.

Parameters were calculated using the equations:

$$\%\ \text{infarct size} = (\text{infarct area}/\text{total LV area}) \times 100$$

$$\%\ \text{infarct thickness} = (\text{anterior wall [infarct thickness]}/\text{septal wall thickness}) \times 100$$

$$\text{viable LV area} = \text{total LV myocardial area} - \text{infarct myocardial area}$$

$$\%\ \text{endocardial infarct length} = (\text{endocardial infarct length}/\text{endocardial LV circumferences}) \times 100$$

$$\%\ \text{epicardial infarct length} = (\text{epicardial infarct length}/\text{epicardial LV circumferences}) \times 100$$

Immunohistochemistry and vascular density. Hearts were fixed in 10% phosphate-buffered formalin. Paraffin-embedded hearts were cut into 5-μm slices. Adjacent sections (taken at the midpoint between LAD ligation site and apex) were stained with rabbit polyclonal antibodies against CD31 or alpha-myosin heavy chain (both from Santa Cruz Biotechnology, Santa Cruz, California), a mouse monoclonal antibody against HIF-1α (Novus Biological, Littleton, Colorado), a mouse monoclonal antibody against VEGFA, or a rabbit polyclonal antibody against iNOS (both from Santa Cruz Biotechnology): 50 sections/heart with 10 sections stained with each antibody, 10 hearts/group [groups: HIF-1α(+)/LAD ligation, HIF-1α(−)/LAD ligation, HIF-1α(+)/sham, and HIF-1α(−)/sham]. Staining for CD31 and iNOS was performed using the Vectastain ABC kit, and the Vector MOM immunodetection kit was used for HIF-1α and VEGFA staining, both according to the manufacturer's instructions (Vector Laboratory, Burlingame, California). The sections were developed in H_2O_2 and diaminobenzidine tetrahydrochloride and counterstained by hematoxylin. Capillary density was expressed as CD31+ endothelial cells per high-power field (200×). Five high-powered fields were counted per section, with 10 sections/heart, and 10 hearts/group. All studies were performed by two independent blinded investigators.

Northern and Western blotting. Northern and Western blotting, including tissue extraction, electrophoresis, and probe labeling, were performed as previously described (13). For Northern blotting, the ^{32}P-labeled probe generated for transgenic HIF-1α spanned base pairs 4895 to 5405 within the α-MHC promoter of the vector construct; while the probe specific for endogenous HIF-1α spanned base pairs 2775 to 3200 of murine HIF-1α mRNA within the 3′ untranslated region. For Northern and Western analysis, infarct tissue was defined as the portion of myocardium that was grossly pale at 24 h or contained visible scar at 4 weeks; peri-infarct tissue was defined as the area of myocardium within 2 mm of the visible edge of infarction; and remote area was taken from the interventricular septum. Infarct, peri-infarct, and regions remote to the infarct were examined independently (5 hearts/group examined at 24 h and 4 weeks after coronary ligation by Northern blot; 5 hearts/group at 24 h and 4 weeks after coronary ligation examined by Western blot). The following antibodies were used: mouse anti-HIF-1α (Novus Biological), mouse anti-VEGFA, rabbit anti-iNOS, and mouse anti-actin (Santa Cruz Biotechnology). Induction of VEGF and iNOS expression was quantified using the IS-1000 digital imaging system (Alpha Innotech Corp., San Leandro, California) with actin band densities serving to normalize protein amounts.

Statistical analysis. Mean ± standard error of the mean (SEM) was reported for each echocardiographic parameter at two time points, 24 h and 4 weeks, within each of the two HIF-1α groups. We compared the HIF-1α(+) and HIF-1α(−) groups with respect to mean magnitude of change from 24 h to 4 weeks after LAD ligation. Student *t* tests were used for comparisons between HIF-1α groups, except for infarct size, for which a Wilcoxon rank sum test was used because normal assumptions did not apply according to a Shapiro-Wilks test. Unadjusted p values are reported for each echo parameter based on the difference between within-animal-group mean changes over time (within-mouse difference between measurement at 4 weeks minus measurement at 24 h). The correlation between echocardiographic and histologic infarct size was tested by linear regression analysis.

RESULTS

To assess the effect of constitutive HIF-1α expression on myocardial infarction and tissue vascularization, we generated transgenic mice lines with full-length murine HIF-1α cDNA under the control of the α-myosin heavy chain (αMHC) promoter (αMHC-HIF-1α) (10). Northern blot analysis of four independent mouse lines generated with the αMHC-HIF-1α transgene demonstrated the presence of transgenic HIF-1α message only in the myocardium and not in other organs, with equal levels of expression in adult atria and ventricles. Morphometric analysis showed normal coronary anatomy and no difference in the number of CD31-stained vascular structures in αMHC-HIF-1α transgenic mice hearts compared with that in age-matched controls under normoxic conditions (data not shown).

We investigated the role of constitutive HIF-1α expression in the setting of acute myocardial infarction. Transgenic and age-matched control mice underwent LAD ligation, followed 24 h and 4 weeks later by M-mode and two-dimensional cardiac echocardiography as well as pathologic and molecular analysis of their hearts. Coronary artery ligation in the mouse produces a broad spectrum of ventricular dysfunction, ranging from mild impairment to overt heart failure. We excluded animals that had akinetic areas more than 50% of the total left ventricular area as detected by echocardiography and clinical signs of heart failure (dyspnea and inability to feed) at 24 h after coronary ligation

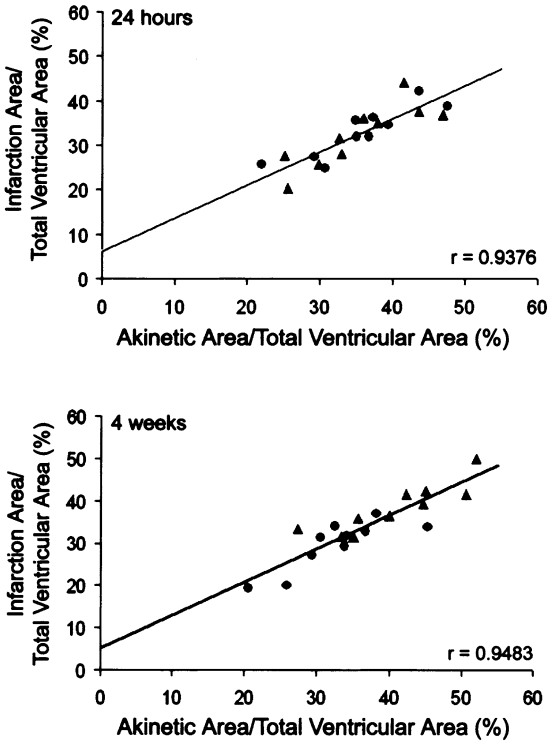

Figure 1. Echocardiographic measurement of akinetic area correlates with pathologic measurement of infarct size at 24 h **(top panel)** and 4 weeks **(bottom panel)** after coronary ligation. Linear regression analysis of the correlation between the percent infarction area/total ventricular area (as measured by TTC or Masson trichrome staining/histology at 24 h and 4 weeks after coronary ligation, respectively) and the percent akinetic area/total ventricular area as measured by two-dimensional echocardiography. For both timepoints n = 20 animals; 10 HIF-1α(+) **(circles)**, 10 HIF-1α(−) **(triangles)**.

from further study. Two additional groups of HIF-1α positive (+) and negative (−) animals underwent sham operation excluding ligation of the LAD artery, followed by echocardiographic, pathologic, and molecular evaluation of their hearts at similar time points.

Correlation between pathologic and echocardiographic measurement of infarct size. Cohorts of animals were sacrificed at 24 h and 4 weeks after coronary ligation to define extent and reproducibility of infarction as well as correlation of acute infarction with echocardiographic parameters (Fig. 1). Twenty-four hours after coronary ligation, HIF-1α(+) and HIF-1α(−) animals demonstrated a similar range of infarction areas (measured as the left ventricular area distinguished by absence of TTC staining) and areas at risk (measured as the left ventricular area excluding retrograde injection of Evans blue dye) (Table 1). Echocardiographic measurement of akinetic area correlated directly with the area of infarction at 24 h and 4 weeks after LAD ligation (Fig. 1). No infarct was detected in sham-operated animals.

Gene expression in infarct, peri-infarct, and septal regions of the heart. We evaluated the expression of HIF-1α in the infarcted heart. Northern blotting using probes specific to either transgenic HIF-1α or endogenous HIF-1α demonstrated two major findings (Fig. 2). First, steady-state levels of *transgenic* HIF-1α mRNA were high throughout atrial and ventricular myocardium in HIF-1α(+) mice under hypoxic and normoxic conditions and not detected in HIF-1α(−) mice. The mRNA levels of transgenic HIF-1α were not affected by hypoxic conditions (Fig. 2). Second, in early infarction (24 h after coronary ligation), levels of *endogenous* HIF-1α mRNA increase three-fold over levels seen under normoxic conditions in both HIF-1α(+) and HIF-1α(−) animals. By 4 weeks after infarction, steady-state levels of endogenous HIF-1α mRNA are low in peri-infarct tissue in both HIF-1α(+) and HIF-1α(−) mice.

By Western blotting, in control HIF-1α(−) infarct animals, HIF-1α protein was detected 24 h after coronary

Table 1. Infarction Changes in LV After MI in HIF-1α(+) and Control Mice

	Infarction Size (%)	AAR (%)	Viable LV Area (mm^2)	Endocardial Infarction Length (%)	Epicardial Infarction Length (%)
24 h					
HIF-1α(+)/LAD ligation (n = 10)	33.4 ± 6.7	36.9 ± 9.8	20.2 ± 4.6	40.1 ± 8.7	32.3 ± 7.2
HIF-1α(−)/LAD ligation (n = 10)	32.0 ± 8.5	36.1 ± 8.2	20.9 ± 4.8	39.8 ± 10.4	32.9 ± 8.8
HIF-1α(+)/sham (n = 5)	—	—	37.2 ± 8.4	—	—
HIF-1α(−)/sham (n = 5)	—	—	36.3 ± 9.3	—	—
		Ant/Septal Wall Thickness (%)			
4 weeks					
HIF-1α(+)/LAD ligation (n = 20)	31.9 ± 4.2†	58.4 ± 9.6*	28.3 ± 3.3*	39.8 ± 10.5†	31.4 ± 8.0
HIF-1α(−)/LAD ligation (n = 20)	40.1 ± 5.3	33.3 ± 4.7	18.1 ± 4.6	50.1 ± 9.2	42.7 ± 7.3
HIF-1α(+)/sham (n = 10)	—	123 ± 28.4	36.4 ± 8.7	—	—
HIF-1α(−)/sham (n = 10)	—	119 ± 29.0	37.8 ± 9.4	—	—

Values indicate mean ± SEM. Parameters were measured on the midline horizontal sections between ligation site and apex of heart. *$p < 0.01$ vs. HIF-1α(−)/LAD ligation group at 4 weeks. †$p < 0.05$ vs. HIF-1α(−)/LAD ligation group at 4 weeks.

AAR (%) = (area at risk/total LV area) × 100; ant/septal wall thickness (%) = (anterior wall (infarct) thickness/septal wall thickness) × 100; endocardial infarction length (%) = (endocardial length of infarction/endocardial LV circumference) × 100; epicardial infarction length (%) = (epicardial length of infarction/epicardial LV circumference) × 100; Infarction size (%) = (infarct area/total LV area) × 100; viable LV area = total LV myocardial area − infarct myocardial area. AAR = area at risk; LAD = left anterior descending coronary artery; LV = left ventricle; MI = myocardial infarction.

JACC Vol. 46, No. 11, 2005
December 6, 2005:2116–24

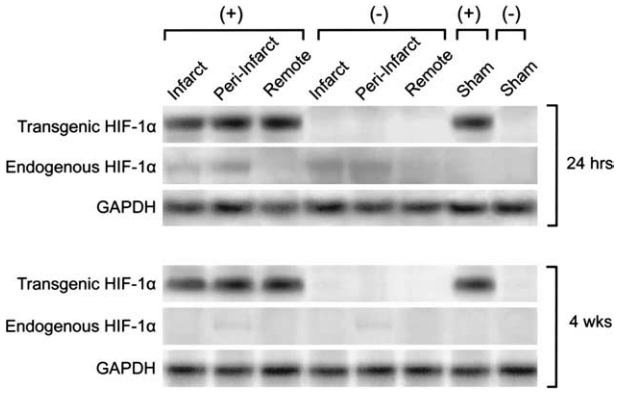

Figure 2. Northern blot analysis of transgenic and endogenous HIF-1α in infarct, peri-infarct, and remote left ventricular regions at 24 h and 4 weeks after LAD ligation and in sham-operated hearts. + = HIF-1α(+) hearts; − = HIF-1α(−) hearts. Steady-state levels of transgenic HIF-1α mRNA are not affected by hypoxic conditions, while steady-state levels of endogenous HIF-1α mRNA are increased in early infarct and peri-infarct regions.

ligation in the peri-infarct and infarct regions (Fig. 3A). At four weeks, HIF-1α was no longer detected in the region of infarction and was expressed at low levels in the peri-infarct region. In contrast, HIF-1α(+) transgenic animals displayed very high levels of HIF-1α protein in infarct and peri-infarct areas immediately after coronary ligation, and this pattern of expression persisted in hearts 4 weeks after infarction.

We confirmed that transgenic HIF-1α is expressed at high levels in cardiomyocytes of the infarcted heart (Fig. 3B) by staining contiguous 5-μm sections with antibodies to HIF-1α and α-MHC (data not shown). We then evaluated two genes whose sequences contain hypoxic response elements and whose transcriptional activity is modulated by HIF in other organ systems: VEGF and iNOS (14, 15). Although HIF-1α(−) infarct animals manifest a two-fold increase in VEGF and iNOS protein in peri-infarct regions compared to noninfarcted septum, HIF-1α(+) infarct animals showed a five-fold increase in VEGF and four-fold increase in iNOS expression in the peri-infarct region compared to nonischemic areas of the heart at both 24 h and 4 weeks after LAD ligation (Fig. 3).

Vascular density measurement. To assess the angiogenic effect of constitutive HIF-1α expression 4 weeks after coronary ligation, we measured vascular density in the peri-infarct (border zone) region adjacent to the infarction, within the infarction, and in the noninfarcted septal region of the left ventricle (Fig. 4). We excised hearts and performed immunohistochemical staining with anti-CD31 antibody to detect endothelial cells. Capillary density observed in the peri-infarct area of the HIF-1α(+) transgenic animals (2,498 ± 277/mm^2) was significantly higher than that of the HIF-1α(−) group (1,015 ± 320/mm^2; $p < 0.01$) and the two sham-operated control groups (HIF-1α(+) sham: 782 ± 194/mm^2; $p < 0.01$; HIF-1α(−) sham: 755 ± 172/mm^2; $p < 0.01$). We observed the increased capillary density caused by transgenic HIF-1α also within the site of infarction. In the septal area that was remote from the infarct site, we observed no difference in vascularity between groups. Angiogenesis in infarct/peri-infarct regions was confined to vessels measuring ≤200 μm in diameter (Fig. 5C).

Cardiac performance 4 weeks after infarction in HIF-1α(+) animals and controls. In the clinical setting, the prevention of progressive heart failure as a result of myocardial infarction is of great importance. To this end, we assessed the cardiac function 4 weeks after myocardial infarction in HIF-1α(+) and HIF-1α(−) mice by echocardiography. The cardiac functional parameters evaluated by echocardiography 4 weeks after LAD ligation are shown in Table 2. In the control group (HIF-1α(−)/coronary liga-

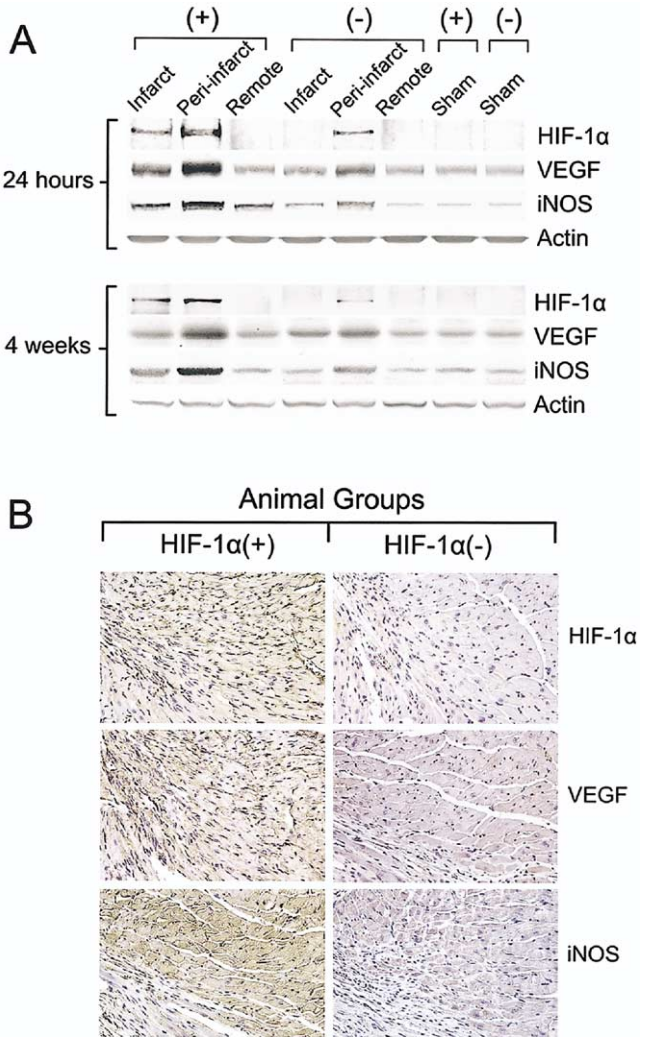

Figure 3. *HIF-1α*(+) transgenic hearts show increased expression of HIF-1α, VEGF, and iNOS in the peri-infarct region compared to control *HIF-1α*(−) hearts. **(A)** Western blot analysis of HIF-1α, VEGF, and iNOS in infarct, peri-infarct, and remote left ventricular regions at 24 h and 4 weeks after LAD ligation and in sham-operated hearts. + = HIF-1α(+) hearts; −= HIF-1α(−) hearts. **(B)** Immunohistochemical localization of HIF-1α, VEGF, and iNOS protein in peri-infarct areas at 4 weeks in HIF-1α(+) and HIF-1α (−) hearts. Sections were counterstained with hematoxylin. Scale bar = 80 μm.

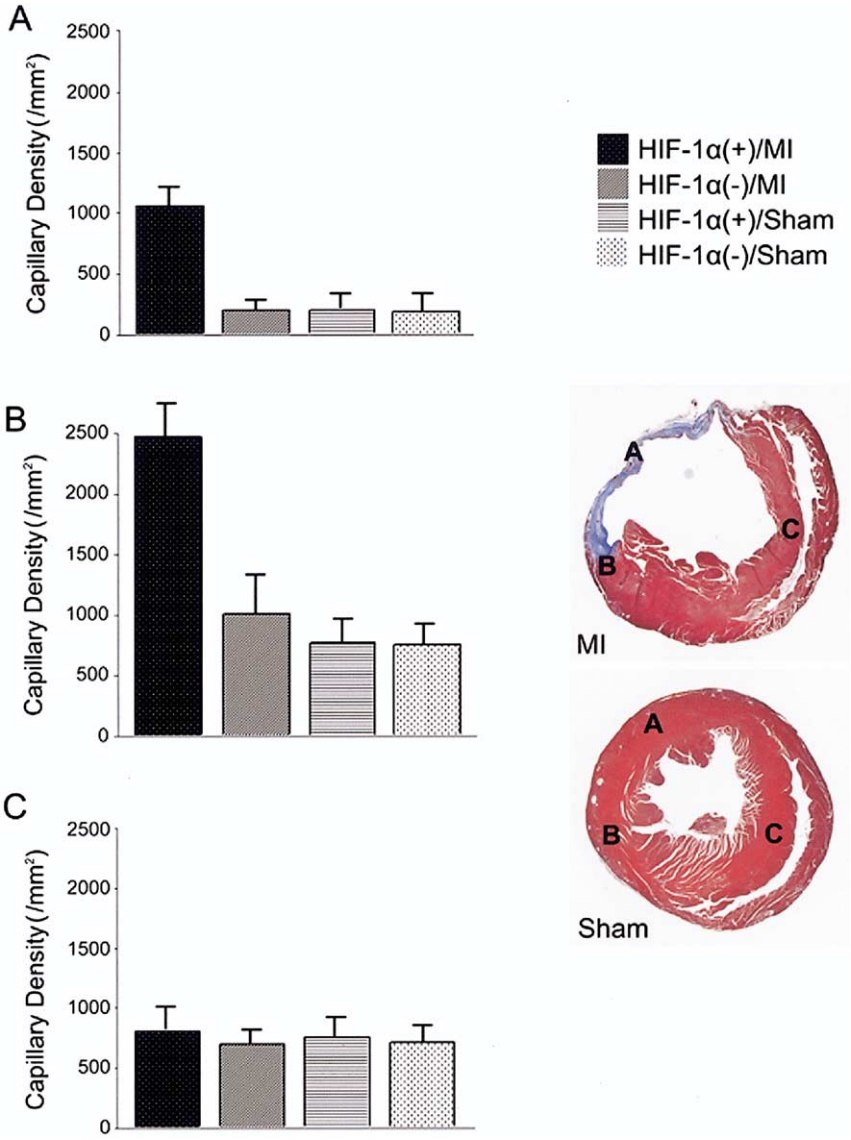

Figure 4. Capillary densities at different locations in the infarcted heart. CD31-positive capillary density was measured at three areas: **(A)** infarction, **(B)** peri-infarct border zone, and **(C)** interventricular septum and similar anatomic areas in sham-operated hearts. The number of CD31-stained capillaries was counted in a blinded fashion and expressed as the number/mm^2. HIF-1α(+)/MI n = 10 animals, HIF-1α(−)/MI n = 10 animals, HIF-1α(+)/sham n = 10 animals, HIF-1α(−)/sham n = 10 animals.

tion), markedly decreased fractional shortening (FS) and ejection fraction (EF) with dilated left ventricular cavity area at diastole (LVAD) and at systole (LVAS) were seen, corresponding to postinfarction myocardial failure. In the HIF-1α(+)/coronary ligation animals, significantly lower LVESD and LVEDD and greater FS and EF were observed compared with the control group (all $p < 0.05$). Sham-operated animals had no evidence of myocardial dysfunction as assessed by echocardiography.

Myocardial pathology 4 weeks after infarction in HIF-1α(+) animals and controls. Microscopic views of trichrome-stained hearts are shown in Figure 5. In HIF-1α(+) and HIF-1α(−) mice that underwent coronary ligation, positively stained fibrous infarcts were found in the heart 4 weeks after myocardial infarction. Thin scars in the area of infarction and dilated left ventricular cavities were observed in the HIF-1α(−) mice. In contrast, hearts in the HIF-1α(+) group had thicker infarcts with partial preservation of cellularity within scar tissue. We measured the infarct size and other parameters in the left ventricles at the section located at the midpoint between ligation and apex (16). Planar morphometric analysis of serial cross-sections showed that despite comparable areas at risk (AARs), the infarct sizes were significantly smaller for the HIF-1α(+) hearts than for the HIF-1α(−) hearts 4 weeks after infarction, and both the percentage of infarct length and that of viable left ventricular area were significantly higher in the HIF-1α(+) group than in the HIF-1α(−) hearts (Table 1, Figs. 5A and 5B). We also tested the effects of constitutive HIF-1α in sham-operated animals to rule out the possibility of a hypertrophic action of HIF-1α under normoxic conditions. No hypertrophy of cardiac muscles

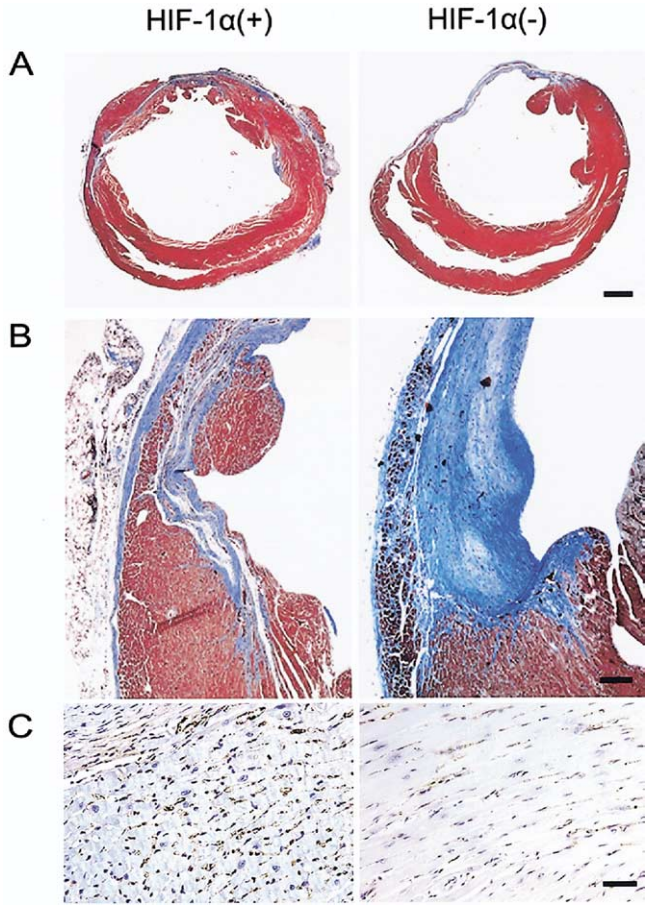

Figure 5. Histology of infarcted hearts. Four weeks after infarction, hearts were excised, sectioned at the level of the papillary muscles, and stained with Masson's trichrome (**A**, scale bar = 1 mm, **B**, scale bar = 200 μm). More preservation of muscular architecture and greater number of peri-infarct vessels seen in *HIF-1α*(+) hearts compared to *HIF-1α*(−) controls. Immunohistochemical staining with anti-CD31 monoclonal antibody in HIF-1α(+) and HIF-1α(−) hearts (n = 10 for each group) 4 weeks after coronary ligation in the peri-infarct region (**C**, scale bar = 45 μm).

was observed in the HIF-1α(+) sham-operated groups (data not shown).

CONCLUSIONS

A critical component of myocardial ischemia is hypoxia, which triggers a wide range of cellular responses, including regulation of gene expression and post-translational modifications of proteins. The pathway for gene regulation in response to hypoxia involves oxygen sensing followed by a series of signal transduction mechanisms that lead to induction or repression of transcription and changes in mRNA stability or the rate of translation or degradation of protein product. In multiple cell culture and animal models, it has been demonstrated that the transcriptional activity, DNA binding capability, and stability of the HIF-1α subunit are directly controlled by intracellular oxygen concentration.

As the rheostat for oxygen sensing in the cell, HIF-1 controls several pathways critical for cellular response to hypoxia. These include: 1) the transcriptional activation of angiogenesis genes such as VEGF, angiopoietin-1 (Ang-1), angiopoietin-2 (Ang-2), placental growth factor, and platelet-derived growth factor beta (17); 2) the recruitment of endothelial progenitor cells to areas of tissue ischemia through an SDF-1-CXCR4 pathway (18); 3) the preconditioning of tissue to tolerate ischemic insult (19,20); 4) the stimulation of solid organ tumor growth (21); and 5) the activation of proinflammatory chemokine production by endothelium through transcriptional modulation of heme oxygenase 1 (22). Indeed, the Semenza group (23) has reported that more than 2% of all human genes are regulated by HIF-1 in human pulmonary artery endothelial cells, confirming the broad range of effects this transcriptional activator has on diverse classes of genes.

The focus of our research is to understand the role of HIF-1 in ischemia and infarction and to characterize the

Table 2. ECHO Parameters of LV Function

Time After Coronary Ligation	HIF-1α(−) (n = 20)		HIF-1α(+) (n = 20)		p Value*
	24 h	4 weeks	24 h	4 weeks	
LAD ligation					
LVEDD (mm)	4.39 ± 0.28	5.99 ± 0.22	4.40 ± 0.13	5.41 ± 0.11	<0.05
LVESD (mm)	3.90 ± 0.29	5.48 ± 0.21	3.88 ± 0.13	4.75 ± 0.12	<0.01
FS (%)	11.6 ± 1.37	8.48 ± 0.61	11.9 ± 1.20	12.3 ± 0.92	<0.05
LVAD (mm^2)	71.4 ± 3.49	73.2 ± 4.45	71.5 ± 4.38	68.2 ± 3.91	<0.05
LVAS (mm^2)	58.2 ± 5.10	55.3 ± 4.36	59.4 ± 4.28	44.0 ± 4.42	<0.01
EF (%)	36.8 ± 6.23	39.3 ± 6.80	34.1 ± 5.34	48.2 ± 4.40	<0.01
Akinetic area (mm^2)	34.2 ± 4.21	41.7 ± 5.81	35.1 ± 5.31	27.5 ± 5.72	<0.01
Sham					
LVEDD (mm)	3.54 ± 0.69	3.52 ± 0.07	3.49 ± 0.08	3.50 ± 0.09	0.43
LVESD (mm)	2.08 ± 0.07	2.11 ± 0.05	2.03 ± 0.09	2.07 ± 0.08	0.83
FS (%)	41.5 ± 1.33	40.1 ± 1.45	42.1 ± 1.02	42.8 ± 1.31	0.64
LVAD (mm^2)	56.4 ± 5.73	57.9 ± 5.36	56.8 ± 6.97	57.1 ± 7.21	0.72
LVAS (mm^2)	25.7 ± 4.70	25.2 ± 5.73	25.8 ± 5.18	25.9 ± 5.37	0.79
EF (%)	71.8 ± 5.28	70.2 ± 4.96	71.2 ± 5.05	71.4 ± 5.77	0.45

Values indicate mean ± SEM. *p Value compares mean magnitude of change from 24 hours to 4 weeks between HIF-1α (+) and HIF-1α (−) groups for each echocardiographic parameter.

EF = ejection fraction; FS = fractional shortening; LV = left ventricle; LVAD = left ventricular area at diastole; LVAS = left ventricular area at systole; LVEDD = left ventricular end-diastolic diameter; LVESD = left ventricular end-systolic diameter.

effect of this gene product on myocardial angiogenesis in normoxic and hypoxic conditions. Our results demonstrate that modulation of the gene target HIF-1α in the heart promoted angiogenesis, led to attenuation of infarct size, and improved cardiac performance after MI in the mouse. We show that overexpression of HIF-1α in our transgenic model allows for supranormal levels of this protein in hypoxic (infarct/peri-infarct) myocardium. This is presumably due to the fact that levels of transgenic HIF-1α protein, stabilized under hypoxic conditions, exceed the known degradation pathway for this protein. Normally, HIF-1α is regulated at the level of protein stability, with a short half-life and rapid ubiquitination in normoxic conditions and a much longer half-life and reduced ubiquitination in hypoxic conditions (24). Hypoxia is also known to trigger transcriptional activation of the endogenous HIF-1α gene within several organs, including human myocardium (2).

Two competing processes modulate the amount of HIF-1α protein in the ischemic heart: production and degradation. We found that under normoxic conditions, transgenic HIF-1α was constitutively expressed at the level of mRNA (promoter expresses transgene regardless of cellular oxygen tension) and endogenous HIF-1α was not expressed. Normal partial pressures of cellular oxygen have been shown to stimulate rapid degradation of the HIF-1α protein. Thus, under normoxic conditions, although HIF-1α was constitutively expressed at the mRNA level in transgenic animals, we found it was barely detectable at the protein level.

In contrast, we found that under hypoxic conditions, transgenic HIF-1α was constitutively expressed at the level of mRNA (promoter expresses transgene regardless of cellular oxygen tension), and endogenous HIF-1α was also expressed. The transcription of the endogenous HIF-1α gene is exquisitely sensitive to the onset of cellular hypoxic conditions, making it one of the earliest effectors of the response to ischemia. Hypoxia led to the stabilization of HIF-1α protein (both transgenic and endogenous) in areas of ischemia, allowing us to measure high levels of HIF-1α protein in infarct and peri-infarct tissue at 24 h after coronary ligation.

In the myocardium of HIF-1α(+) mice, a marked increase in blood vessels in the peri-infarct and infarct regions was observed. Sufficient blood flow as a result of this increased blood vessel formation might be instrumental to prevention of the loss of cardiomyocytes in these zones over time, preservation of contractility in the border zone adjacent to the infarct, and suppression of postinfarction cardiac failure during left ventricular remodeling. Myocardial deterioration after infarction in HIF-1α(+) animals may be limited, not only as a result of stimulation of angiogenesis through a VEGF-related pathway, but also through additional HIF-1–mediated local adaptations to low oxygen tension, such as recruitment of scaffolding progenitor cells, vasodilatation through an iNOS-related pathway, protection from oxidant stress, and a transition to anaerobic metabolism.

So far, efforts to stimulate angiogenic response in the heart have been limited to the introduction of exogenous growth factors such as fibroblast growth factors (FGFs) or VEGFs (25,26) and stabilizing proteins such as VP-16 and PR39 (27,28) by means of gene or protein delivery. Our report suggests the possibility of using the α-subunit of the transcriptional enhancer HIF-1 alone to stimulate angiogenic response to hypoxia, without the known reported side effects of excessive unregulated myocardial VEGF, such as fragile and immature vessels, angioma formation, and elicitation of systemic hypotension (29,30).

In summary, although multiple genes undoubtedly contribute to remodeling of the left ventricle after infarction, we show that a single gene, HIF-1α, induces therapeutic angiogenesis, limits infarct size, and improves myocardial function after acute coronary occlusion. Our results may have important practical implications for the treatment of patients with severe myocardial ischemia.

Reprint requests and correspondence: Dr. Patricia A. Thistlethwaite, Division of Cardiothoracic Surgery, University of California, San Diego, San Diego, California 92103-8892. E-mail: pthistlethwaite@ucsd.edu.

REFERENCES

1. American Heart Association. Heart Disease and Stroke Statistics: 2004 Update. Dallas, TX: American Heart Association, 2003.
2. Lee SH, Wolf PL, Escudero R, Deutsch R, Jamieson SW, Thistlethwaite PA. Early expression of angiogenesis factors in acute myocardial ischemia and infarction. N Engl J Med 2000;342:626–33.
3. Wang GL, Jiang BH, Rue EA, Semenza GL. Hypoxia-inducible factor 1 is a basic-helix-loop-helix-PAS heterodimer regulated by cellular O_2 tension. Proc Natl Acad Sci U S A 1995;92:5510–14.
4. Maxwell PH, Wiesener MS, Chang GW, et al. The tumour suppressor protein VHL targets hypoxia-inducible factors for oxygen-dependent proteolysis. Nature 1999;399:271–75.
5. Cockman ME, Masson N, Mole DR, et al. Hypoxia inducible factor-alpha binding and ubiquitylation by the von Hippel-Lindau tumor suppressor protein. J Biol Chem 2000;275:25733–41.
6. Forsythe JA, Jiang BH, Iyer NV, et al. Activation of vascular endothelial growth factor gene transcription by hypoxia-inducible factor 1. Mol Cell Biol 1996;16:4604–13.
7. Jung F, Palmer LA, Zhou N, Johns RA. Hypoxic regulation of inducible nitric oxide synthase via hypoxia inducible factor-1 in cardiac myocytes. Circ Res 2000;86:319–25.
8. Ang SO, Chen H, Hirota K, et al. Disruption of oxygen homeostasis underlies congenital Chuvash polycythemia. Nat Genet 2002;32:614–21.
9. Goda N, Ryan HE, Khadivi B, McNulty W, Rickert RC, Johnson RS. Hypoxia-inducible factor 1alpha is essential for cell cycle arrest during hypoxia. Mol Cell Biol 2003;23:359–69.
10. Ng WA, Grupp IL, Subramaniam A, Robbins J. Cardiac myosin heavy chain mRNA expression and myocardial function in the mouse heart. Circ Res 1991;68:1742–50.
11. Sjaastad I, Sejersted OM, Ilebekk A, Bjornerheim R. Echocardiographic criteria for detection of postinfarction congestive heart failure in rats. J Appl Physiol 2000;89:1445–54.
12. Melo LG, Agrawal R, Zhang L, et al. Gene therapy strategy for long-term myocardial protection using adeno-associated virus-mediated delivery of heme oxygenase gene. Circulation 2002;105:602–7.
13. Sullivan CC, Du L, Chu D, et al. Induction of pulmonary hypertension by an angiopoietin 1/TIE2/serotonin pathway. Proc Natl Acad Sci U S A 2003;100:12331–6.
14. Skinner HD, Zheng JZ, Fang J, Agani F, Jiang BH. Vascular endothelial growth factor transcriptional activation is mediated by

hypoxia-inducible factor 1alpha, HDM2, and p70S6K1 in response to phosphatidylinositol 3-kinase/AKT signaling. J Biol Chem 2004;279:45643–51.
15. Tendler DS, Bao C, Wang T, et al. Intersection of interferon and hypoxia signal transduction pathways in nitric oxide-induced tumor apoptosis. Cancer Res 2001;61:3682–8.
16. Takahashi K, Ito Y, Morikawa M, et al. Adenoviral-delivered angiopoietin-1 reduces the infarction and attenuates the progression of cardiac dysfunction in the rat model of acute myocardial infarction. Mol Ther 2003;8:584–92.
17. Semenza GL. Angiogenesis in ischemic and neoplastic disorders. Ann Rev Med 2003;54:17–28.
18. Ceradini DJ, Kulkarni AR, Callaghan MJ, et al. Progenitor cell trafficking is regulated by hypoxic gradients through HIF-1 induction of SDF-1. Nat Med 2004;10:858–64.
19. Semenza GL. O_2-regulated gene expression: transcriptional control of cardiorespiratory physiology by HIF-1. J Appl Physiol 2004;96: 1173–7.
20. Date T, Mochizuki S, Belanger AJ, et al. Expression of constitutively stable hybrid hypoxia-inducible factor-1a protects cultured rat cardiomyocytes against simulated ischemia-reperfusion injury. Am J Physiol Cell Physiol 2005;288:C314–20.
21. Korkolopoulou P, Patsouris E, Konstantinidou AD, et al. Hypoxia-inducible factor 1alpha/vascular endothelial growth factor axis in astrocytomas. Associations with microvessel morphometry, proliferation and prognosis. Neuropathol Appl Neurobiol 2004;30:267–78.
22. Ockaili R, Natarajan R, Salloum F, et al. HIF-1 activation attenuates post-ischemic myocardial injury: a role for heme oxygenase-1 in modulating microvascular chemokine generation. Am J Physiol Heart Circ Physiol 2005;289:H542–8.
23. Manalo DJ, Rowan A, Lavoie T, et al. Transcriptional regulation of vascular endothelial cell responses to hypoxia by HIF-1. Blood 2005; 105:659–69.
24. Baek JH, Mahon PC, Oh J, et al. OS-9 interacts with hypoxia-inducible factor 1α and prolyl hydroxylases to promote oxygen-dependent degradation of HIF-1α. Mol Cell 2005;17:503–12.
25. Giordano FJ, Ping P, McKirnan MD, et al. Intracoronary gene transfer of fibroblast growth factor-5 increases blood flow and contractile function in an ischemic region of the heart. Nat Med 1996;2:534–9.
26. Su H, Lu R, Kan YW. Adeno-associated viral vector-mediated vascular endothelial growth factor gene transfer induces neovascular formation in ischemic heart. Proc Natl Acad Sci U S A 2000;97: 13801–6.
27. Shyu KG, Wang MT, Wang BW, et al. Intramyocardial injection of naked DNA encoding HIF-1alpha/VP16 hybrid to enhance angiogenesis in an acute myocardial infarction model in the rat. Cardiovasc Res 2002;54:576–83.
28. Li J, Post M, Volk R, et al. PR39, a peptide regulator of angiogenesis. Nat Med 2000;6:49–55.
29. Lopez JJ, Laham RJ, Carrozza JP, et al. Hemodynamic effects of intracoronary VEGF delivery: evidence of tachyphylaxis and NO dependence of response. Am J Physiol 1997;273:H1317–23.
30. Carmeliet P. VEGF gene therapy: stimulating angiogenesis or angioma-genesis? Nat Med 2000;10:1102–3.